Disclaimer:

The contents of this report reflect the views of the authors, who are responsible for the facts and the accuracy of the information presented herein. This document is disseminated in the interest of information exchange. The report is funded, partially or entirely, under 69A3552348333 from the U.S. Department of Transportation's University Transportation Centers Program. The U.S. Government assumes no liability for the contents or use thereof.

Transportation Infrastructure Precast Innovation Center (TRANS-IPIC)

University Transportation Center (UTC)

3D-Printed Advanced Materials to Mitigate Prestressed Concrete Girder End Cracks
UB-23-RP-02

FINAL REPORT

Submitted by:
Ravi Ranade, Associate Professor, ranade@buffalo.edu
Department of Civil, Structural and Environmental Engineering
University at Buffalo

Co-PIs: Chi Zhou (chizhou@buffalo.edu) and Pinar Okumus (pinaroku@buffalo.edu), University at Buffalo

Collaborators / Partners:
None

Submitted to:
TRANS-IPIC UTC
University of Illinois Urbana-Champaign
Urbana, IL

Executive Summary

Efficient bridge girder sections with thinner and deeper webs are prone to end zone cracks during prestress release, raising potential durability concerns. Reasons for these cracks include the transfer of large prestressing forces over a short distance and the low tensile strain capacity of concrete. Commonly adopted measures to mitigate these cracks include special detailing in the anchorage zones and several measures for detensioning and handling these girders. While these structural approaches provide some crack mitigation, a more effective solution is needed to address the underlying problems of concrete's low tensile strain capacity and inability to restrain crack widths. This report investigates using cover shells, made of advanced concrete materials with enhanced tensile strain capacity, at girder ends to mitigate surface cracks. Additionally, the report explores the integration of the proposed solution into the precast manufacturing process using 3D-printing-based methods, aiming for minimal changes to existing workflows.

Objectives:

- To investigate the feasibility of using strain-hardening cementitious composites (SHCC) cover shells for mitigating end cracking in precast-prestressed concrete beams.
- To develop a 3D-printable SHCC and appropriate printing parameters for the above application.
- To understand the composite action between SHCC shells and conventional concrete.

Methodology:

- A nonlinear finite element analysis (FEA) is conducted to evaluate the material strain capacity demands for mitigating girder end zone cracks.
- An experimental protocol is utilized to develop and optimize an SHCC for 3D-printing.
- A small-scale gantry-type 3D concrete printer is constructed using generic parts and open-source firmware components.
- A four-point bending test is employed to assess the preliminary feasibility of the proposed solution preliminarily.

Key findings and recommendations:

- The FEA of an example prestressed concrete girder showed that the maximum tensile strain on the exterior surface at the girder end is approximately 0.32%. Based on this result and accounting for variations in material properties, the target tensile strain capacity for developing a 3D-printed SHCC was taken as 0.6%. The FEA-based approach presented in the report can be more broadly employed to establish target material properties for a given application.
- Flowability factor and flow reduction rate were used to quantify and assess the printability of a given SHCC with a given printing system. For nozzle size of 0.76 in. or greater, SHCC materials with a flowability factor between 1.2-1.5 and flow reduction rate >20% per hour were found printable.
- A modular, three-component 3D concrete printer with pumping, gantry, and control systems was developed. A high-torque motor with a screw-based extruder was found suitable for pumping and extruding SHCC. G-code optimization was used to compensate for the lack of control over the pumping system.
- The four-point bending tests of beams with and without 3D-printed SHCC covers are in progress, and this report will be updated or supplemented with additional findings after these tests are complete.

Table of Contents

TRANS-IPIC Final Report

Statement of problem

Precast-prestressed concrete bridge girders are susceptible to cracking at their ends, as shown in Figure 1 [1]. Transfer of large prestress forces to concrete over a short length causes high tensile strains at the girder ends. This, combined with conventional concrete's brittleness and low tensile strain capacity, leads to end cracking, which is a major concern for bridge owners as these cracks, especially those near the bottom of the beam, might not close under live load. Such cracks could facilitate rapid chloride penetration and lead to corrosion of the prestressing strands or rebars and deterioration of the girder's load capacity.

Literature suggests various crack control strategies for prestressed girder ends, which can be classified as (i) design and handling-based strategies [2-6] and (ii) materials-based strategies [7, 8]. Design-based strategies rely on end-zone reinforcement pattern adjustments, debonding strands at ends, and following an optimized order of strand cutting at prestress transfer. Furthermore, removal, lowering, and spreading out of draped strands reduce the cracking strains at girder ends. On the other hand, material-based strategies utilize advanced concrete materials, such as ultra-high performance concrete (UHPC) [9] and strain-hardening cementitious composites (SHCC) [10], with significantly higher tensile strain capacity than conventional concrete to control girder end cracking [7, 8].

Although advanced concrete materials can be used for the entire girder, it might not be practical due to non-standard design provisions, higher costs, and limited data on these materials' time-dependent properties. Limiting the use of advanced concrete materials like SHCC to replace ordinary concrete only at the girder ends might appear appropriate but could pose implementation issues. Therefore, as an alternative method to achieve efficient cross-sections and to protect girder ends against end zone cracking, the present study proposes a novel approach of utilizing 3D-printed SHCC covers as a permanent formwork to bridge girders. The approach efficiently limits the construction efforts to an SHCC cover, mitigating the need for the entire end sections with SHCC. Figure 1 shows a concept SHCC cover at the girder end.

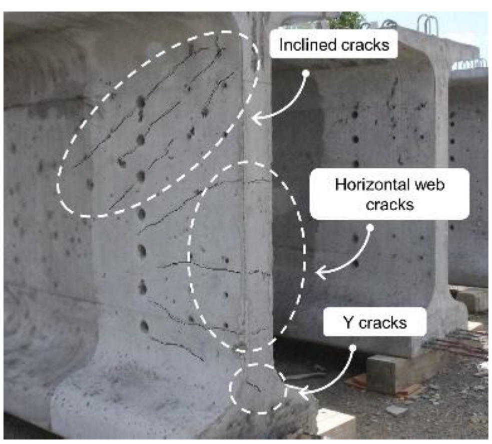

(a)

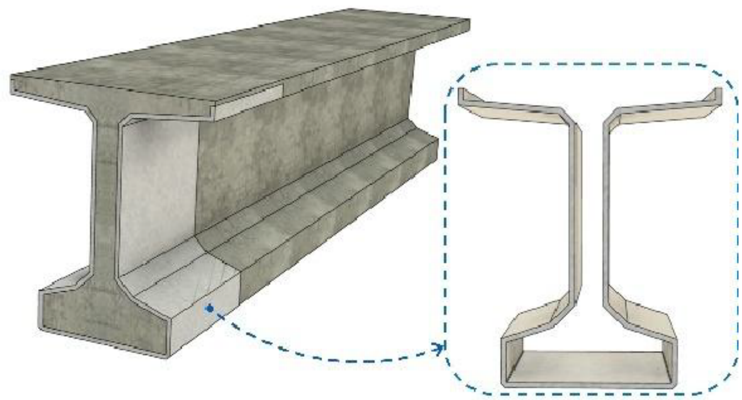

(b)

Figure 1. (a) Typical cracks in the end zone of a pretensioned bulb tee girder [1] (b) 3D-printed SHCC covers as permanent formwork at girder ends

With the overall goal of addressing the problem of girder end cracking through improvement in materials and construction technology, the specific objectives of this study are as follows:

1. To investigate the feasibility of using SHCC shells for mitigating end cracking in precast-prestressed concrete beams,
2. To develop a 3D-printable SHCC and appropriate printing parameters for the above application,
3. To understand the level of composite action between SHCC shells and conventional concrete.

Research tasks

The following research tasks were performed to meet the above objectives:

Task 1: Numerical simulation of pretensioned beams with SHCC shells at the end zone (100% completed)

Task 1 involved simulating a prestressed concrete bridge girder numerically to determine the maximum tensile strain in concrete at girder ends and understand the effects of the material properties and structural parameters on end cracking. A nonlinear finite element model of a standard Tx70 girder was developed using the software ABAQUS. The structural design of the beam, including cross-section, prestressing force, and reinforcement detailing, was adopted from experiments performed by O'Callaghan and Bayrak [11]. The element type and size in the numerical simulation were calibrated to match the transverse reinforcement strains observed by O'Callaghan and Bayrak [11] at the end zone of the concrete girder. Based on this calibration, a 50 mm element size was selected for numerical modeling. Subsequently, a 0.75" SHCC cover at the end zones was applied in the numerical model, keeping all other parameters constant. A representative finite element model and observed surface strain profile of the simulated girder end with SHCC cover are shown in Figure 2.

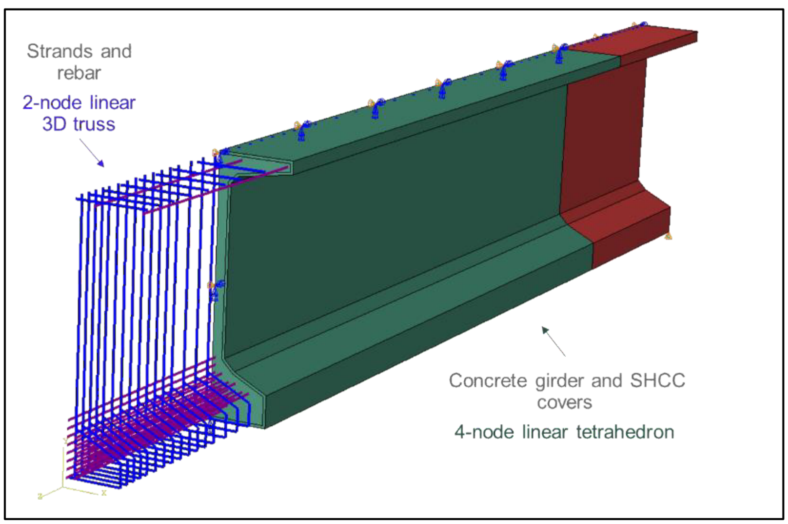

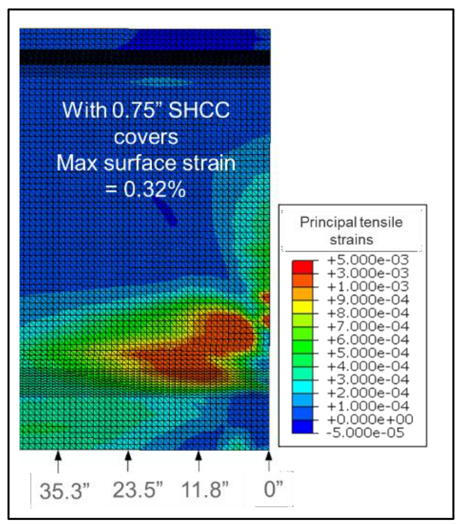

Figure 2. (a) Representative fine element model (b) Surface strain profile at girder end with SHCC cover

Appropriate material models for conventional concrete, SHCC, strands, and rebars were selected. Conventional concrete was modeled using the concrete damage plasticity model available in ABAQUS, SHCC was modeled using a trilinear model, and rebar and strands were modeled using bilinear models. Two-node linear 3D truss elements were adopted for strands and rebars. The concrete girder and SHCC cover were modeled using 4-node linear tetrahedron elements. Rebar and prestressing strands were embedded in the girder. The prestressing force was simulated through temperature strain applied to the strands. The interface between the SHCC cover and the concrete girder was modeled with tie constraints.

Based on the numerical analysis, the maximum tensile strain on the surface at the girder end was computed as 0.32%. Additionally, the analysis indicated that a 0.75″ thick SHCC cover did not significantly affect the tensile stress in the longitudinal reinforcement within the anchorage zone. This suggests that using thin SHCC covers will not alter the structural design of these girders.

Task 2.1: Determination of target material properties for a printable SHCC
(100% completed)

Task 2.1 entailed determining the target material properties needed to enable the 3D printing of SHCC covers for the prestressed girder application. The performance requirements for SHCC were categorized into two groups: (i) fresh state requirements and (ii) hardened state requirements. The fresh state requirements were established for the following five steps of material production and printing:

i. Mixing: Mixing capacity, in terms of the maximum shear rate that the concrete mixer can apply, was considered for determining the target matrix viscosity needed for homogeneous fiber dispersion.
ii. Pumping (Pump): The rheological properties of the SHCC mixture were tuned, and appropriate pumping equipment (motor) was selected to enable continuous pumping while preventing fiber clumping and segregation.
iii. Pumping (Pipe): The rheological properties of the SHCC mixture were also adjusted, and an appropriate diameter and type of pipe were selected to prevent blockage and segregation in the pipe.
iv. Extrusion (Nozzle): Blockage at the nozzle and filament tear was minimized by controlling the material's rheological properties and using a customized nozzle (printed separately by the investigators).
v. Layering: Shape retention of layers was achieved by considering the setting characteristics and flow reduction rates of SHCC mixtures.

It was observed that the above steps require contrasting rheological characteristics, as shown in Figure 3. For example, a highly viscous mix is good for fiber dispersion, segregation prevention, and filament tearing prevention, but it might cause issues in mixing and pumping due to the available equipment's capacity limitations. High viscosity also increases the risk of blockage during pumping and extrusion.

A flow table test (ASTM C1437) [12] based on relative rheological characterization was implemented in this task due to its simplicity and strong correlations with materials yield stress and viscosity. The flow table test was used to determine two parameters: (i) Flowability factor and (ii) Flow reduction rate. Flowability factor [13] is defined as the ratio of the diameter of the fresh material sample after 25 drops of the flow table test [12] to the base diameter of the flow cone (100 mm). The flow reduction rate measures the reduction in fresh material's flowability (or thixotropy) over time. Both these rheological properties are essential to assess the printability of the material. Suitable ranges of these two parameters were identified for tailoring SHCC mixtures. Further details of the testing procedure are presented below under Task 2.3.

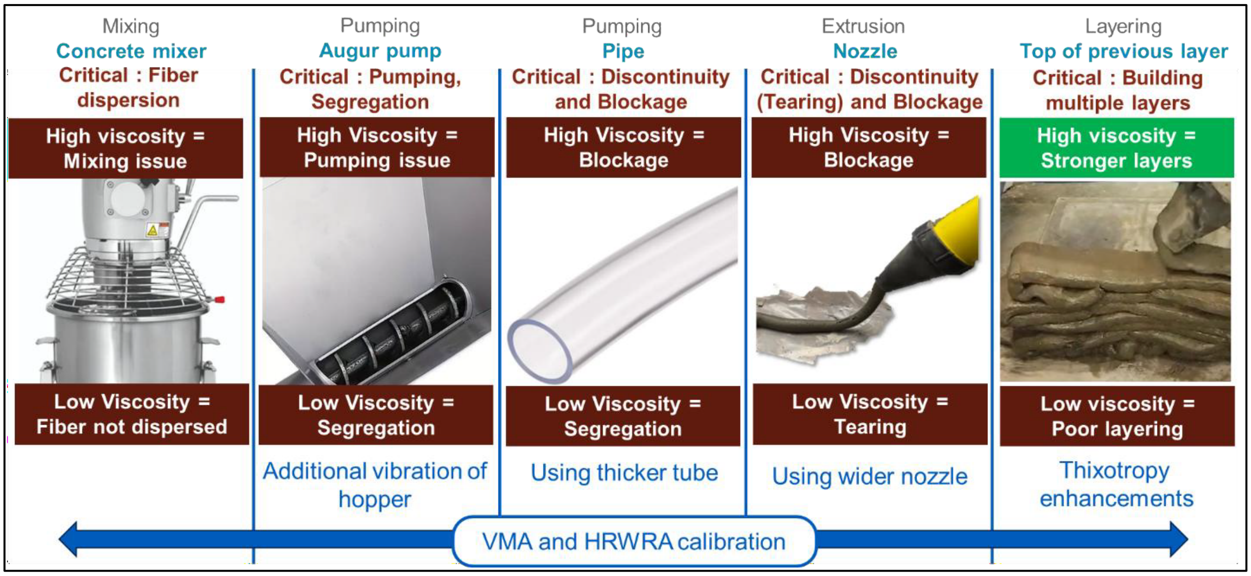

Figure 3. Contrasting rheological requirements from mixing to printing of SHCC

The target mechanical properties for developing a 3D-printable SHCC in the hardened state for the given application included compressive strength and tensile strain capacity. As the compressive strength of conventional concrete used in bridge girders typically exceeds 6 ksi, the same value was used as the lower bound for the SHCC's compressive strength. Based on the numerical model results of task 1, the minimum tensile strain capacity for the SHCC was 0.32%. However, a higher strain capacity of 0.6% was targeted to account for material variability.

Thus, the following material property requirements were identified through this task:

Fresh state requirements (flow table test):

i. Flowability factor (slump diameter after 25 drops/original diameter) = 1.2 to 1.5; for the 0.76" or bigger nozzle size
ii. Flow reduction rate (average percentage decrease rate in flowability factor in first 30 min) > 20% per hour

Hardened state requirements:

i. Compressive strength > 6 ksi
ii. Tensile strain capacity > 0.6%

Task 2.2: Trial mix designs
(100% completed)

This task involved developing preliminary SHCC mixture compositions suitable for 3D-printing with the target properties determined in Task 2.1. An SHCC mixture with high tensile strain capacity but lacking printability, developed previously in PI's lab, was adopted as the baseline. Iterative modifications to the mix were performed as follows to make it 3D-printable:

i. Reduction in water/cementitious material (w/cm) weight ratio: The flow of the baseline SHCC mix was too high for 3D printing. Therefore, as the first step, the w/cm ratio was reduced from 0.38 (in the baseline mixture) to 0.31 to reduce the flow and enhance the compressive strength.
ii. Use of 8mm PVA fibers: The length of polyvinyl alcohol (PVA) fibers was reduced from 12mm (in the baseline mixture) to 8mm to enhance the pumping and extrusion of the mixture.
iii. Adjusting chemical admixtures dosages: The quantities of High Range Water Reducing Admixture (HRWRA) and Viscosity Modifying Admixture (VMA) were adjusted to achieve the target fresh state characteristics identified in task 2.1. Sixteen mixtures with varying combinations of VMA and HRWRA amounts were prepared and screened using the flowability factors and flow reduction rates. Out of these 16 combinations, four mixtures were found suitable for further optimization.
iv. Enhancement of thixotropic behavior: The mixtures selected in the previous step were further optimized to increase their flow reduction rate. Ingredients like micro silica, ground silica, and type III cement were incorporated into the mix, and the fresh state behavior was investigated. Based on the trials performed, three mixtures were selected for further evaluation. The details of these mixtures and mix design procedure can be found in Figure 4 and the conference paper referenced below.

The outcome of this task was three SHCC mixtures suitable for 3D printing applications.

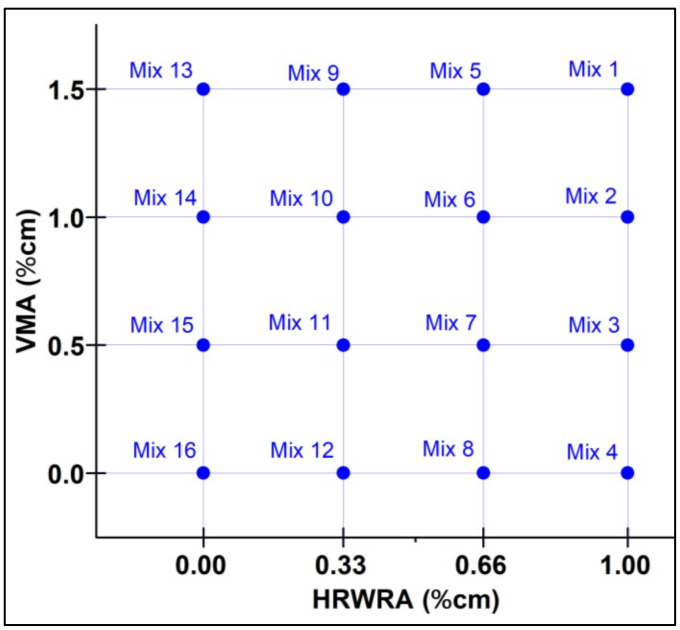

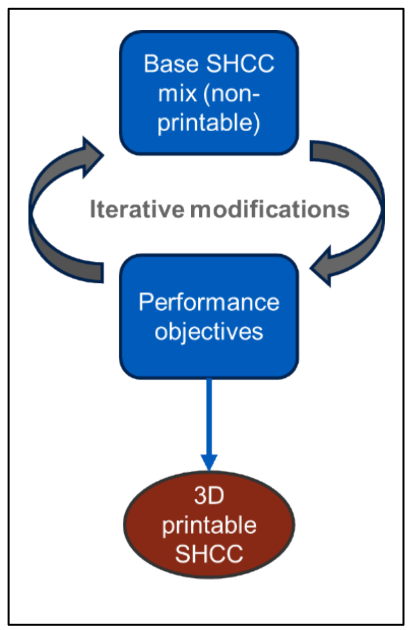

Figure 4. (a) Trial mixtures for rheology optimization of SHCC (b) Iterative mix design procedure

Task 2.3: Fresh and hardened properties testing
(100% completed)

Investigations of the fresh and hardened properties of the three mixtures developed in the previous task were performed in task 2.3. This task was performed iteratively with tasks 2.1 and 2.2.

Fresh state screening was performed using a caulking gun and flow table test to reject non-printable mixtures. This screening was performed using qualitative and quantitative criteria, as shown in Figure 5 and described below:

i. Fiber dispersion was checked by hand to determine if there was fiber clumping. The mixtures with observable fiber clumps were rejected.
ii. A grout caulking gun with a nozzle size of approximately 0.76″ was employed to access the extrudability. Mixes that failed to extrude from this caulking gun were rejected.
iii. Buildability/shape retention: Multiple layers of material were built using a caulking gun. If a mix failed to take the weight of at least one layer over it, it was rejected.
iv. For relative quantification of the rheological behavior of the developed mix, a flow table test was conducted immediately after mixing and then 30 minutes later to determine flow reduction with time.
v. After each flow table test, the mixtures were observed for segregation/water bleeding, and the mixtures with observable segregation/water bleeding were rejected.

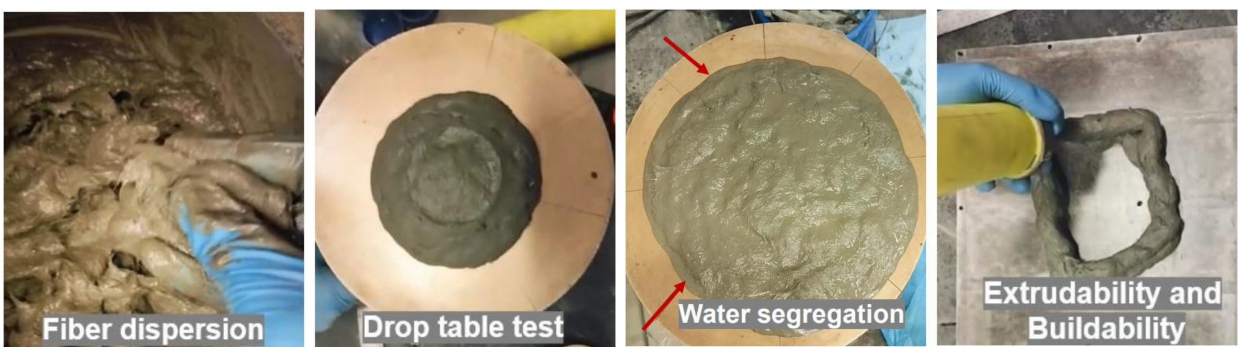

Figure 5. Mix screening protocol based on fresh properties

Hardened properties tests of the screened mixtures were performed. These tests included compressive strength (ASTM C109 [14]), direct tension [15], and four-point flexure tests (ASTM C78 [16]). After initial screening and optimization, three mixtures were selected (as described in task 2.2) for further evaluation. Table 1 summarizes the hardened properties of the three 3D printable SHCC mixtures (M9-MS, M9-IS, and M10). Representative tensile stress-strain behaviors and bending stress-deflection response for mixtures M9-MS, M9-IS, and M10 are shown in Figures 6 and 7, respectively.

Table 1. Hardened properties of 3D printable SHCC mixtures (COV = coefficient of variation)

Mix	Compressive strength		Tensile strength (Direct tension test)		Modulus of rupture (4-point bend test)	
	Mean (ksi)	COV (%)	Mean (ksi)	COV (%)	Mean (ksi)	COV (%)
M9-IS	7.5	5.6	0.8	19.0	1.5	12.5
M9-MS	8.5	2.4	0.7	17.5	1.5	8.0
M10	8.2	5.6	0.9	15.1	1.3	8.4

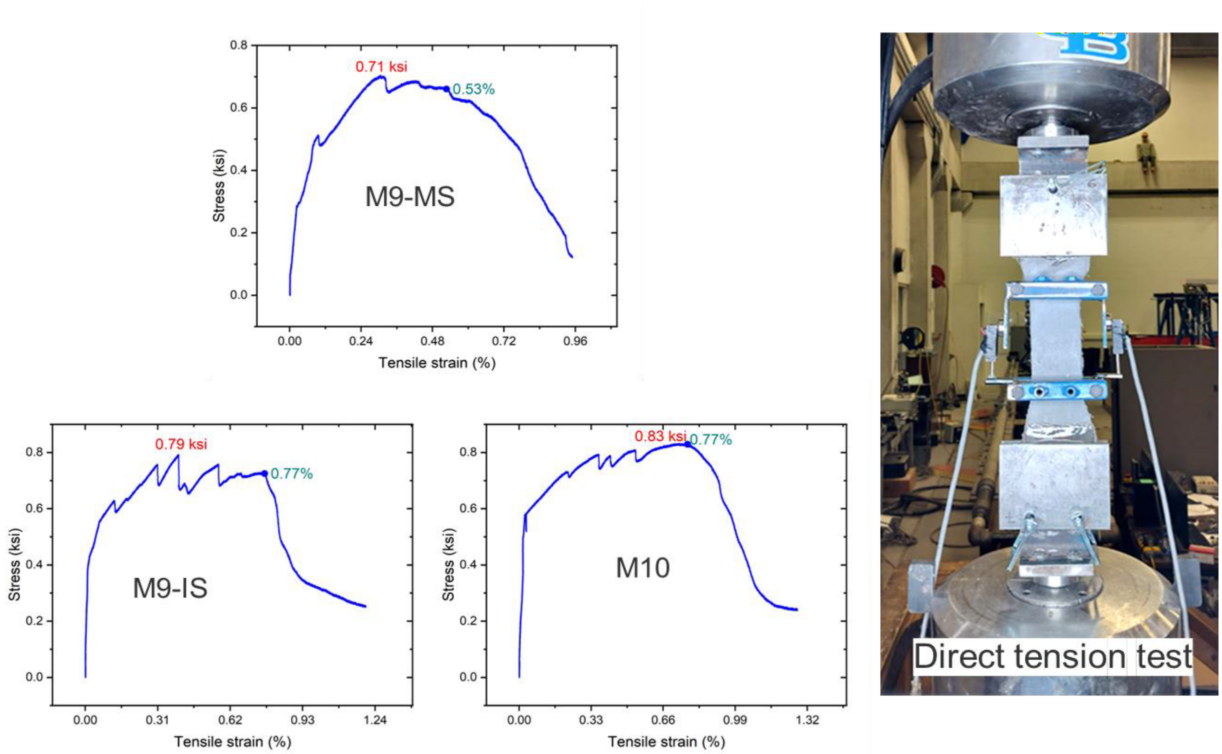

Figure 6. Stress-strain response of 3D printable SHCC mixtures under direct tension.

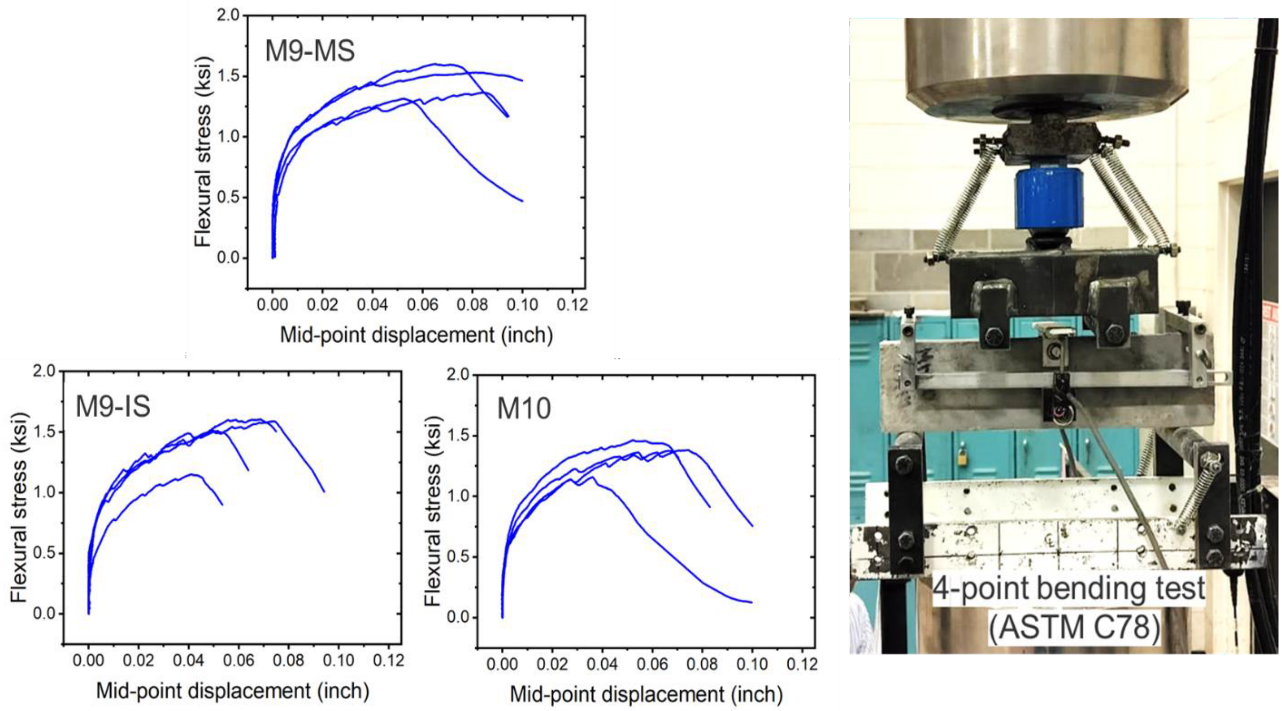

Figure 7. Flexural stress-midpoint deflection response of 3D printable SHCC mixtures under four-point bending.

Task 2.4: Mixture refinement
(100% completed)

In this task on mixture refinement, the above three printable SHCC mixtures (M9-MS, M9-IS, and M10) were further modified to investigate the effect of fly ash/cement weight ratio on printability and strain hardening behavior. Six new mixture compositions (2 variations for each mixture) were developed, and their hardened properties, including compressive (following ASTM C109 [14]) and direct tensile behaviors [15], were evaluated. Table 2 summarizes the hardened properties of the modified SHCC mixtures.

With the increase in fly ash content in the SHCC mixtures, a marginal decline in 28-day compressive strength was observed. On the contrary, the tensile strain capacity showed an increasing trend with increased fly ash content. However, the variation in results (COV) was too high to draw definitive conclusions. Although an elaborate quantification of the flow behavior was not performed, it was observed that the mix flowability was too high for the fly ash/cement weight ratio of 1.8, indicating the need for rheological re-optimization for 3D printing application at such a high proportion of fly ash in the mixture. Considering the need for rheological re-optimization, the modified mixtures were not considered for use in the composite beam tests planned in Tasks 3.1 and 3.2.

Table 2. Hardened properties of modified 3D printable SHCC mixtures

SHCC Mix	Fly ash to cement weight ratio	Compressive strength		Tensile strength (from direct tension test)		Tensile strain capacity	
		Mean (ksi)	COV (%)	Mean (ksi)	COV (%)	Mean (%)	COV (%)
M9-IS	1.2 (Base)	7.5	5.6	0.8	19.0	0.7	22.6
	1.5	6.4	12.8	0.7	4.8	1.4	17.4
	1.8	6.3	12.5	0.7	2.0	2.1	17.2
M9-MS	1.2 (Base)	8.5	2.4	0.7	17.5	0.6	27.0
	1.5	8.7	6.8	0.9	1.3	1.3	23.1
	1.8	8.1	6.9	1.0	8.3	1.9	47.4
M10	1.2 (Base)	8.2	5.6	0.9	15.1	0.9	58.3
	1.5	7.2	5.1	0.9	5.6	1.7	10.2
	1.8	6.3	1.5	0.8	1.2	1.9	14.1

Task 3.1: Preparation of composite beam specimens with 3D-printed SHCC shells
(100% completed)

This task aimed to evaluate the performance of SHCC covers as permanent formwork in mitigating the surface cracks developed in conventional concrete beams. The task involved multiple subtasks, as discussed below:

1. <u>Conventional concrete mix design</u>: For our planned experimentation, a conventional concrete mix design was adopted from O'Callaghan and Bayrak [11]. Adjustments were made to account for the available raw materials, and the resulting mix design is given in Table 3. With a w/c ratio of 0.35, a compressive strength of 5.6 ksi was achieved 24 hours since casting. The aggregate and cement properties are given in Table 4, and the moisture contents of aggregates are presented in Table 5.

Table 3. Conventional concrete mix

Material	lb/cyd
Coarse aggregate (SSD)	1709
Fine Aggregate (SSD)	1343
Cement (Type III)	700
Water	245
High Range Water Reducing Admixture, HRWRA	12 oz/Cwt

Table 4. Material properties for conventional concrete mix

Fine aggregates:	
Fineness modulus	3.74
Bulk specific gravity in SSD state	2.40
Coarse aggregates:	
Nominal maximum aggregate size	0.5"
Bulk specific gravity in SSD state	2.60
Cement:	Type III

Table 5. Moisture content of aggregates used in conventional concrete

	Moisture content (%)	
	Natural	SSD
Coarse aggregates	0.56	0.74
Fine aggregates	4.40	2.40

2. Cross-section design: Considering the scope of the project, a trial section for a rectangular beam was designed. The objectives for the design were to achieve a beam section with reasonable rebar sizes and a small (considering 3D printer size, testing equipment capabilities, minimizing material waste minimization) but sufficient cross-sectional area to accommodate a 3D-printed SHCC shell and a conventional concrete layer in the cover zone. Additionally, the beam was required to fail in flexure as the SHCC cover is intended for use in the flexural cracking zone. With these underlying objectives, multiple cross-sections were explored, and the selected section is shown in Figure 8. The section has a U-shaped 3D-printed SHCC shell of thickness equal to 0.8″ in the cover zone. A clear spacing of 0.7″ between the 3D-printed cover and stirrups is given to reduce any hindrance to aggregate flow around the stirrup. Two No.4 rebars are used as main reinforcement. Additionally, No.3 rebars with 3″ center to center spacing in shear critical zones and 6″ center to center spacing in non-critical zones are employed as stirrups to maintain shear load capacity more than twice the flexural load capacity of the beam.

3. 3D-printing of SHCC cover: An SHCC cover was printed using the M9-MS 3D-printable SHCC mixture developed in Task 2.2. As a first step, the printer parameters for the adopted material were optimized to achieve suitable printing. Initial iterations were performed to print a multi-layered wall using the selected mixture, adjusting different feed rates and offset distances. The objective was to avoid under-extrusion or scraping (over-extrusion) while printing, as shown in Figure 9. Once finely printed layers were achieved, the cover was printed.

Additionally, our laboratory's existing continuous extrusion system creates material buildup at the ends while printing a U-shape. This problem will be resolved and will not be observed with commercial printers. But for now, a rectangular SHCC cover with five sides was 3D-printed, and two sides were cut off to create a U-shaped cover.

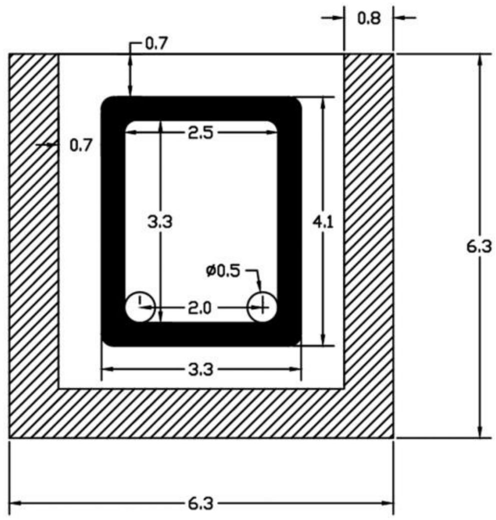

Figure 8. Cross-section of planned beam for testing (all dimensions in inches rounded to first decimal place).

Figure 9. Machine-material interaction parameters optimization: (a) Under-extrusion (b) Over-extrusion (Scraping) (c) Printing with optimized parameters.

4. <u>Concrete casting</u>: For the considered cross-section, two beam specimens are prepared. The first specimen is a control beam without any SHCC cover in the flexural zone but with the same cross-section and reinforcement, as shown in Figure 8. Another specimen is the beam with a 3D-printed SHCC cover. Additionally, the integration of the 3D-printed cover into the precast workflow was considered while minimizing the required changes. Therefore, a proposed implementation procedure for manufacturing precast girders with 3D-printed covers is planned. Further, a similar workflow is developed for casting reinforced concrete beams to be tested in the present study. The proposed workflow and sequence of steps in casting girders for structural testing are shown in Figure 10.

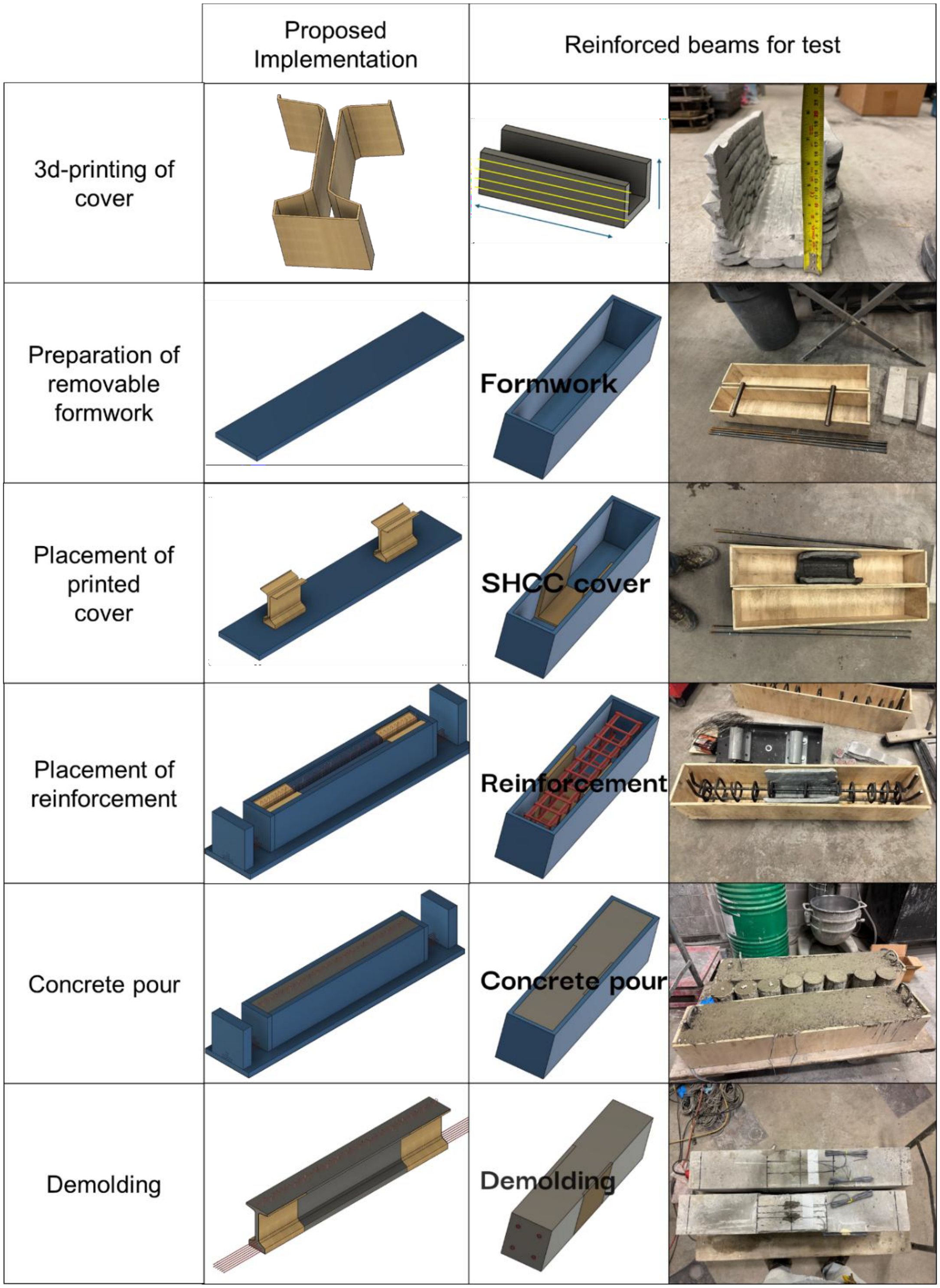

Figure 10. Proposed methodology to integrate 3D-printed cover into precast workflow and casting of reinforced beam with similar procedure.

Task 3.2: Testing of beams under mechanical loading
(Ongoing)

This task involves testing the beam specimens prepared in Task 3.1, as shown in Figure 11. A test setup for the beams and accompanying instrumentation is being planned and prepared. The beams will be tested using a four-point bend setup, as shown in Figure 11.

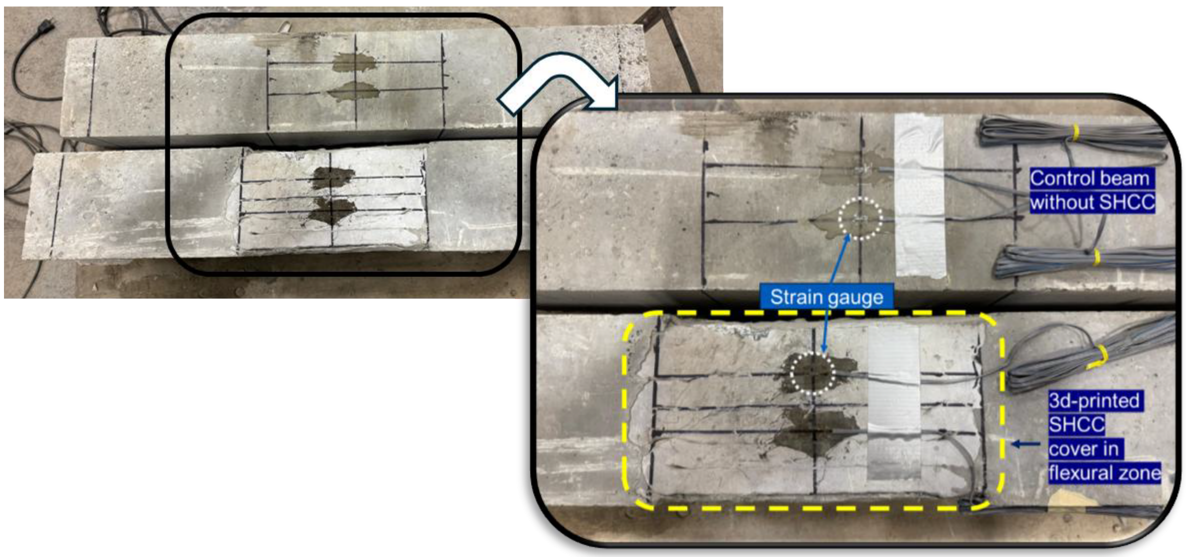

Figure 11. Beam specimens for testing under four-point bend test (bottom surface)

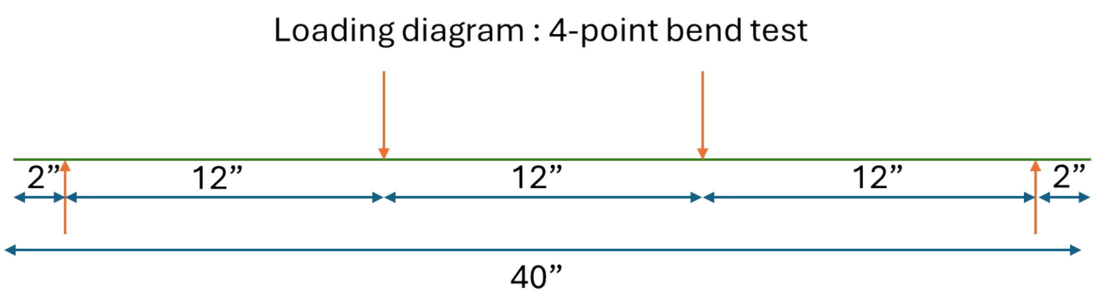

Figure 12. Loading diagram for beam testing

Educational outreach activities

The project activities have been demonstrated through the following educational outreach events:

1. UB Science Exploration Day on March 20th, 2024, University at Buffalo, NY.
2. Structural Engineering and Earthquake Simulation Laboratory (SEESL) outreach on November 12th, 2024, University at Buffalo, NY.
3. SEESL outreach on November 19th, 2024, University at Buffalo, NY.
   The photographs below were taken at these outreach activities.

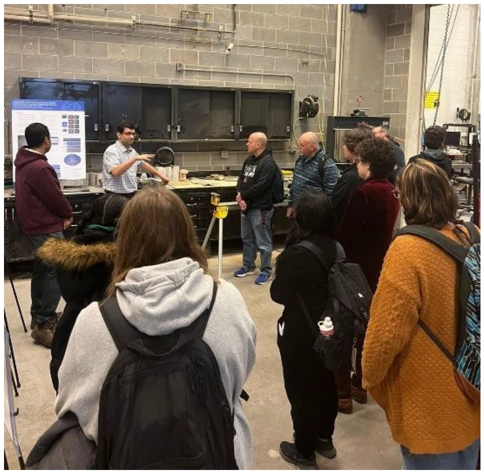

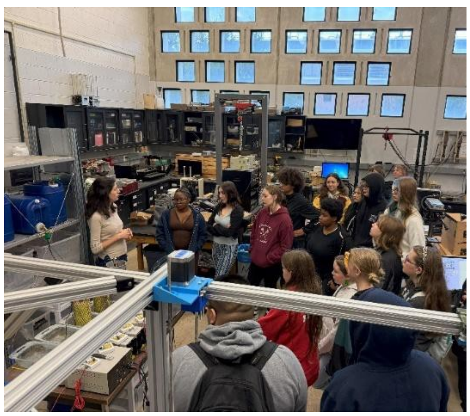

Workforce development activities

1. One new undergraduate research intern worked on the project in the summer of 2024. Working alongside the graduate student, he gained vital skills in mixing, processing, casting, testing, and printing fiber-reinforced concrete materials. The undergraduate intern also performed a feasibility study on applying artificial neural networks to deduce fundamental rheological properties of SHCC based on the results of rheometer experiments.

2. A key outcome of this research is the method for developing a printable SHCC. The material development process and the applications of the material to bridges are included in a lecture in the PI's graduate course on Advanced Concrete Materials, which is taught every Fall semester at the University at Buffalo.

Technology transfer actions

None

Papers

1. Peer-reviewed conference paper at BEFIB 2024 – XI International symposium on fiber reinforced concrete. 15-18 September 2024, Dresden, Germany, pp. 451-458.
DOI: 10.1007/978-3-031-70145-0_55.

Authors: Singh, P., Gadde, V.S., Zhou, C., Okumus, P., and Ranade, R.
Title: Development of 3D printable strain-hardening cementitious composites for bridge-related applications”.

Presentations and posters

1. Poster presentation at the Annual meeting of the Transportation Research Board (TRB) in Washington, D.C. from January 7-11, 2024. Authors: Singh, P., Gadde, V.S., Zhou, C., Okumus, P., and Ranade, R. Title: 3D printed advanced materials to mitigate prestressed concrete girder end cracks.
2. Presentation to the UB Institute of Bridge Engineering External Advisory Board, which consists of current and past DOT officials, practicing engineers, and UB alums, April 30, 2024, Buffalo, NY. Authors: Singh, P., Gadde, V.S., Zhou, C., Okumus, P., and Ranade, R. Title: 3D Printed Advanced Materials to Mitigate Prestressed Concrete Girder End Cracks.
3. Presentation at conference BEFIB 2024 XI International symposium on fiber reinforced concrete. 15-18 September 2024, Dresden, Germany. Authors: Singh, P., Gadde, V.S., Zhou, C., Okumus, P., and Ranade, R., Title: Development of 3D printable strain hardening cementitious composites for bridge-related applications
4. Poster presentation at Summer School of the Research Training Group GRK 2250 “Mineral-bonded composites for enhanced structural impact safety” 18-20 September 2024, Dresden, Germany. Authors: Singh, P., Landge, S.D., Zhou, C., Okumus, P., and Ranade, R., Title: 3D printed SHCC as permanent formwork for crack width control in prestressed precast concrete bridge girders.
5. Extended abstract and Presentation at TRB AAMCT 2024 – Transportation Research Board Conference on Advancing Additive Manufacturing and Construction in Transportation, November, 2024. Authors: Singh, P., Gadde, V.S., Zhou, C., Okumus, P., and Ranade, R. Title: Development of 3D printable strain hardening cementitious composites for bridge-related applications

Other events

None

TRANS-IPIC news items

None

References

[1] P. Okumus, R. P. Kristam, and M. Diaz Arancibia, "Sources of Crack Growth in Pretensioned Concrete-Bridge Girder Anchorage Zones after Detensioning," *Journal of Bridge Engineering,* vol. 21, no. 10, 2016, doi: 10.1061/(asce)be.1943-5592.0000928.

[2] P. Gergely and M. A. Sozen, "Design of Anchorage-Zone Reinforcement in Prestressed Concrete Beams," *PCI Journal,* vol. 12, no. 2, pp. 63-75, 1967, doi: 10.15554/pcij.04011967.63.75.

[3] J. Kannel, C. French, and H. Stolarski, "Release Methodology of Strands to Reduce End Cracking in Pretensioned Concrete Girders," *PCI Journal,* vol. 42, no. 1, pp. 42-54, 1997, doi: 10.15554/pcij.01011997.42.54.

[4] W. T. Marshall and A. H. Mattock, "Control of Horizontal Cracking in the Ends of Pretensioned Prestressed Concrete Girders," *PCI Journal,* vol. 7, no. 5, pp. 56-74, 1962, doi: 10.15554/pcij.10011962.56.74.

[5] B. E. Ross, H. R. Hamilton, and G. R. Consolazio, "Experimental and Analytical Evaluations of Confinement Reinforcement in Pretensioned Concrete Beams," *Transportation Research Record: Journal of the Transportation Research Board,* vol. 2251, no. 1, pp. 59-67, 2011, doi: 10.3141/2251-06.
[6] C. Y. Tuan, S. A. Yehia, N. Jongpitaksseel, and M. K. Tadros, "End Zone Reinforcement for Pretensioned Concrete Girders," *PCI Journal,* vol. 49, no. 3, pp. 68-82, 2004, doi: 10.15554/pcij.05012004.68.82.
[7] H. Li, L. Li, X. Fan, M. Ye, X. Shao, and L. Yi, "Experimental and numerical investigation on the flexural behavior of a large-scale prestressed UHPC T-Shaped girder," *Engineering Structures,* vol. 272, 2022, doi: 10.1016/j.engstruct.2022.115027.
[8] V. S. Ronanki, S. Aaleti, and J. P. Binard, "Long-Span Hybrid Precast Concrete Bridge Girder Using Ultra-High-Performance Concrete and Normalweight Concrete," *PCI Journal,* vol. 64, no. 6, 2019, doi: 10.15554/pcij64.6-02.
[9] K. Ragalwar, W. F. Heard, B. A. Williams, and R. Ranade, "Significance of the particle size distribution modulus for strain-hardening-ultra-high performance concrete (SH-UHPC) matrix design," *Construction and Building Materials,* vol. 234, 2020, doi: 10.1016/j.conbuildmat.2019.117423.
[10] V. C. Li, "On Engineered Cementitious Composites: A Review of the Material and its Applications," *J. Adv. Concr. Technol.,* vol. 1, no. 3, pp. 215-230, 2003.
[11] M. R. O'Callaghan and O. Bayrak, "Tensile stresses in the end regions of pretensioned I-beams at release," THE UNIVERSITY OF TEXAS AT AUSTIN 2008.
[12] "ASTM C1437, Standard test method for flow of hydraulic cement mortar."
[13] D. G. Soltan and V. C. Li, "A self-reinforced cementitious composite for building-scale 3D printing," *Cement and Concrete Composites,* vol. 90, pp. 1-13, 2018, doi: 10.1016/j.cemconcomp.2018.03.017.
[14] "ASTM C109, Standard Test Method for Compressive Strength of Hydraulic Cement Mortars (Using 2-in. or [50-mm] Cube Specimens)."
[15] D. Kumar and R. Ranade, "Influence of matrix-modification and fiber-hybridization on high-temperature residual mechanical performance of strain-hardening cementitious composites," *Construction and Building Materials,* vol. 302, 2021, doi: 10.1016/j.conbuildmat.2021.124157.
[16] "ASTM C78, Standard Test Method for Flexural Strength of Concrete (Using Simple Beam with Third-Point Loading)."